



ELSEVIER

Available online at www.sciencedirect.com

SCIENCE @ DIRECT®

Journal of Colloid and Interface Science ●●● (●●●●) ●●●-●●●

JOURNAL OF
Colloid and
Interface Science

www.elsevier.com/locate/jcis

Morphology control of poly(vinylidene fluoride) thin film made with electrospray

Ivo B. Rietveld^{a,b,*}, K. Kobayashi^{a,b}, H. Yamada^a, K. Matsushige^a^a Department of Electronic Science and Engineering, Kyoto University, A1-326, Katsura, Nishikyo-ku, Kyoto 615-8510, Japan^b International Innovation Center, Kyoto University, Katsura, Nishikyo-ku, Kyoto 615-8520, Japan

Received 6 October 2005; accepted 19 December 2005

Abstract

Thin polymer films of poly(vinylidene fluoride) were prepared with electrospray. Effects of solvent, initial spray concentration, temperature, solution conductivity, and polymer size on the film morphology were studied with AFM. The two main factors controlling polymer film morphology are the droplet size of the spray and the viscosity of the solution at deposition. These factors determine the flow of the polymer-solvent mixture over the substrate, the density of the film, and its smoothness. The solvent is a key parameter of the entire process. It affects spray stability, polymer solubility, droplet size of the spray, and viscosity of the solution at deposition. Solvents with a low vapor pressure provide a wider window for optimization of other parameters and are therefore preferred over solvents with high vapor pressure. The viscosity at deposition is mainly controlled with the initial spray concentration, polymer size, temperature, and droplet size. The droplet size is best controlled by the conductivity of the solution and the flow rate of the spray.

© 2005 Elsevier Inc. All rights reserved.

Keywords: Poly(vinylidene fluoride); Thin film; Electrospray; Electrohydrodynamic atomization; Polymer; Morphology control; Electrospray deposition

1. Introduction

Interest in electrospray, also known as electrohydrodynamic atomization, has been present for centuries; a liquid under influence of a high electric field is drawn into the direction of the field and may emit droplets. If the electric field is strong enough, a cone appears from which a mist of very fine droplets emanates; the so-called cone-jet, first theoretically described by Taylor [1]. Despite the interest, applications with electrospray have not been manifold for a long time. In the late eighties Cloupeau et al. [2–4] gave one of the first thorough empirical descriptions of the conditions of cone-jet formation. One of the most important applications was developed around the same time, electrospray mass spectroscopy by Fenn [5] to produce single, charged molecules for mass analysis. In the nineties many more empirical and theoretical studies of electrospray followed, mainly focused on aerosol technology [6–15].

Interest grew in electrospray preparation of thin films [16–18] and electrospray of polymers [19,20], which were logically combined in electrospray studies for film and coatings prepared with polymers [21–28]. Fabrication of thin polymer films is difficult due to the large molecular size and properties like chain entanglement and high viscosity. As a result of the high solution viscosity two types of polymer electrospray evolved: polymer coatings by regular electrospray [21–25] and electrospinning [26–28]. With regular electrospray, small polymer particles are formed from dilute concentrations which fuse on the substrate into a continuous film.

Poly(vinylidene fluoride), PVDF, led to a specific interest in the usage of electrospray. PVDF is a ferroelectric polymer and its ferroelectricity is dependent on the crystal structure of the polymer [29]. The ferroelectric crystal structure can be induced by applying very high electric fields (MV/cm). Electrospray requires high electric fields and has been successfully combined with the fabrication of ferroelectric PVDF films [21,22,30]. Ferroelectricity makes PVDF an interesting material for ultra-thin films prepared under precisely controlled conditions. Moreover PVDF is a relatively inert polymer, which makes it a suitable

* Corresponding author. Fax: +81 75 383 2308.

E-mail address: rietveld@piezo.kuee.kyoto-u.ac.jp (I.B. Rietveld).

candidate for thin coatings. Both properties led to the use of PVDF in this study.

Despite the growing interest in polymer electrospray, only recently a few surface morphology studies based on SEM images have appeared, analyzing surface morphology of electrosprayed polymer films as a function of several parameters [31–33]. In one paper a thorough account is given on the effect of solvent, voltage (or charge), flow rate, and concentration on a biological polymer [31]. Also a paper on the precise control of quantity and location appeared [34]. However, precise control of polymer film morphology is not well-understood yet. Especially the production of nanometer thick polymer films is still difficult, due to the multitude of parameters that affect the electrospray result. The aim of this paper is therefore to single out the parameters, which are the most convenient to control polymer film morphology.

Polymer film morphology in terms of smoothness and strength (network formation) depends on the polymer particle size and the spread of polymer on the substrate. Smaller spray droplets will result in smaller particles and a smoother film. A certain level of restricted flow will promote network formation of the polymers; high droplet viscosity on the substrate will result in a film of dry, loose polymer particles, and low viscosity will result in polymer, being washed away from the substrate. A precise control of the interplay between droplet size, particle size, and viscosity is, therefore, the key to control the film morphology.

An advantage of electrospray is the fact that the droplet size can be controlled. On the other hand, many parameters influence the electrospray process and therefore also the droplet size. The parameters which control the electrospray process and the parameters which determine the droplet size are known and their relationships have been well studied [9,10,15]. This is important, because an analysis of these studies will allow a systematic choice of parameters that need to be thoroughly investigated for polymer film production. Of course, other parameters might still have an influence on spray stability, but that is thoroughly studied in the previously cited studies and many other references therein [4,10,35,36].

Ganan-Calvo used an analytical approach to extend Taylor's electrostatic solution [1] and obtained an expression for the current (I), transferred by the droplets in the electrospray process, as a function of the flow rate (Q) and the conductivity (K) of the sprayed liquid [9]:

$$I = 4.25 \left[\frac{QK\gamma}{\ln(Q\rho K/\gamma\varepsilon_0)^{1/2}} \right]^{1/2}, \quad (1)$$

where γ is the surface tension, ρ is the density of the sprayed liquid, and ε_0 is the vacuum permittivity constant. Equation (1) was obtained under the condition that the jet emanating from the cone was thin enough in diameter to have a flat velocity profile; the liquid velocity at the surface of the jet has to be of the same order as in the center of the jet. The scaling law proved to be applicable to a wide range of different liquids [9].

The analytical approach of Ganan-Calvo does not contain droplet break-up; therefore it cannot determine the size of the droplet on a pure theoretical basis. It can, however, determine

the diameter of the jet at the estimated position of break-up, which is related to the droplet diameter (d) [9]:

$$d = 3.78\pi^{-2/3} \left(\frac{\rho\varepsilon_0 Q^3}{\gamma K} \right)^{1/6} f_b, \quad (2)$$

where f_b is the nondimensional radius of the jet at break-up and a constant value of 0.6 provides reasonable fits with a variety of literature data [9].

Hartman et al. derived a similar but simpler current scaling law for a flat velocity profile in the jet [36]:

$$I \sim (\gamma QK)^{1/2}. \quad (3)$$

Hartman et al. also derived a scaling law for the droplet diameter [15]:

$$d \sim \left(\frac{\rho\varepsilon_0 Q^4}{I^2} \right)^{1/6}. \quad (4)$$

It is important to note that Eq. (4) is valid irrespective of a flat velocity profile in the jet. If a flat profile is present, Eq. (3) can be substituted into Eq. (4), resulting in Eq. (2). Prefactors are not given in the references of Hartman et al. [15,36].

Hartman et al. also identifies two break-up regimes for the jet, the varicose break-up, and the whipping jet break-up. Since the latter regime has a broader droplet size distribution, varicose break-up is preferred in applications. The whipping jet regime occurs when the ratio of the normal electric stress and the surface tension exceeds 0.3. This ratio is difficult to determine in practice, because precise knowledge of the droplet velocity at jet break-up is necessary. The droplet size in the whipping jet regime, however, is limited by the electric stress and can be calculated with the use of the Rayleigh limit of electric charge on a droplet [15]:

$$d = \left(0.8 \frac{288\varepsilon_0\gamma Q^2}{I^2} \right)^{1/3}. \quad (5)$$

The factor 0.8 is according to Hartman the best value for the droplet stress ratio. Which equation to apply can be determined by comparison of the results of Eqs. (4) and (5); the one yielding the smallest droplet size is the correct equation. It also indicates if the jet is in the varicose mode or the whipping mode [15].

The equations provide the parameters that can be changed to adjust the size of the droplet and of the resulting polymer particle in the droplet. The two most obvious parameters to use are the conductivity and the flow rate. The other variables are solvent properties (density, surface tension, or dielectric constant), which cannot be changed separately. In this paper the solution conductivity was chosen to control the droplet size, since flow rate together with the electric field and some solvent properties were reserved to control spray stability. It is known that the electric field also influences the droplet size [14], but the effect is small and can be explained in terms of flow rate and conductivity [15].

The solution viscosity is completely absent from the scaling relationships. Although viscosity has a strong influence on the presence of a flat velocity profile [10], necessary for the validity of Eqs. (1)–(3), the validity may be ensured over a wide

viscosity range due to the small diameter of the jet [9]. Furthermore, Hartman et al. studied the effect of viscosity on the development of the jet. It appears that viscosity increases the wavelength of the varicose fluctuation on the jet. The size of the wavelength is proportional to the droplet size. However, viscosity also slows down the jet break-up (compare to electrospinning, where break-up does not occur at all), resulting in a thinner jet. The thinner jet and the larger varicose wavelength seem to compensate each other, resulting in comparable droplet sizes under similar conditions for liquids with a wide range of viscosities (0.4–20 mPa s) [15]. Although the role of the viscosity is not completely resolved, one can conclude that Eqs. (1)–(4) will apply for dilute polymer solutions that have a viscosity between 0.5 and 10 mPa s.

The surface tension is not solely a solvent property, since it can be modified by surfactants. However, surfactants are not effective in the cone-jet process. Static surface tension induced by surfactants establishes in the order of seconds, due to the necessary molecular rearrangements at the surface of a liquid [37,38]. Electrospay is a fast dynamic process in a steady state, where processes take place in microseconds or faster [15,39]. Since this is not a static equilibrium situation, static equilibrium surface tension cannot apply. The surface tension will be mainly depending on the major compound, the solvent, with a value which may deviate from its own static equilibrium value.

The foregoing discussion has reduced the suitable parameters to control the droplet size, to flow rate and liquid conductivity. The main objective of this study becomes therefore how to control the viscosity of the droplet at deposition, while controlling the droplet size of the spray with the liquid conductivity. The main and very important requirement in this paper is a stable cone-jet spray, which highly depends on the variables of Eqs. (1)–(4). The cone-jet is in general stable for a specific range of conductivity and flow. More about spray stability can be found in Refs. [4,10,15,35, and references therein].

In the following sections a study of PVDF films with AFM and thickness profiling is presented. In a few cases infrared spectroscopy was used to determine the presence of solvent in the films. The effect of concentration, spray distance, spray time, size (polymer-oligomer), temperature, conductivity, and solvent on the film morphology is discussed.

2. Materials and methods

Poly(vinylidene fluoride) was purchased from Sigma–Aldrich, $M_w = 534,000$ g/mol. *N,N*-dimethylformamide 99.7% and acetone 99.5% were obtained from Nacalai Tesque, Japan. VDF-oligomer, $M_w = 1982$ g/mol, was provided by Daikin, Japan. Ammonium nitrate 99.0% was purchased from Wako Ltd., Japan. All chemicals have been used as purchased. Silicon wafer was used as substrate (resistance = 1–5 Ω cm), purchased from E&M, Japan. Wafers were all cleaned before use with acetone in an ultrasonic bath for at least 15 min.

Polymer solutions were made by weighing the appropriate amount of polymer in DMF or acetone. After an ultrasonic treatment of 30 min, the solutions were allowed to dissolve for at least one night. Solutions with increased conductivity were

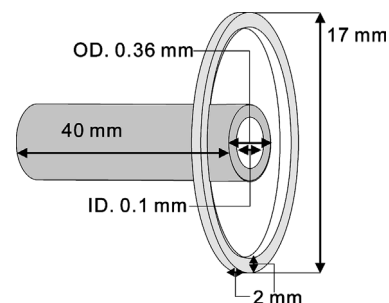


Fig. 1. The ring is positioned at the tip of the nozzle. The ring and nozzle in the drawing are not to scale. The diameter of the metal ring is 17 mm and its thickness is 2 mm. The outer diameter of the nozzle is 0.36 mm, the inner diameter is 0.36 mm, and the total length of the nozzle is 40 mm. The potential of the ring is 3.0 kV. The potential of the nozzle is adjusted as indicated in the text.

prepared by dissolving the appropriate amount of ammonium nitrate in DMF and were subsequently used for the preparation of polymer solution. The conductivity was checked with a Horiba pH conductometer D-54 and the Horiba conductivity cell 3551.

The films were prepared with an in-house constructed electrospay chamber. The capillary, made of stainless steel, has an outer diameter 0.36 mm and an inner diameter 0.1 mm with a flat tip. The tip of the capillary has been placed in the center of a thin metal ring (2 mm thick) with a diameter 1.7 cm, as shown in Fig. 1. The capillary is perpendicular to the plane of the ring, which has a constant potential 3.0 kV. A potential range 0–20 kV can be applied to the capillary, with positive bias. The sample holder can be displaced from 0 to 12 cm from the capillary. The sample holder is connected to ground via a currentmeter. The current was monitored during every experiment with a Keithley 6517 electrometer. A constant liquid flow was provided with a syringe pump Model 22 of Harvard apparatus. High potential was supplied with devices constructed in-house and containing Ultravolt Inc. voltage supply modules.

The liquid flow rate during the experiments was 2 μ l/min for DMF and 3 μ l/min for acetone. Flow rate was used in combination with the potential to ensure a stable cone-jet. The voltage range for a stable cone-jet spray shifts slightly with distance and with sprayed solution; in the case of DMF for 1 cm the range is 5.15–5.60 kV, for 2 cm 5.30–5.75 kV, and for 4 cm 5.55–6.10 kV, in the case of acetone for 2 cm the range is 4.60–5.00 kV. A stable cone-jet spray exists within these ranges. Outside the given ranges a cone-jet can exist, however it may be prone to fluctuations. Samples with high conductivity needed on average a 0.3 kV higher potential to ensure a stable spray, than the volt-ranges mentioned above. The spray stability was tested before the actual film production and if necessary, the potential was slightly adjusted in accordance with the distance and conductivity.

The films were prepared in a nitrogen atmosphere with a humidity level of 5% or lower, because a constant humidity appeared to be of great importance to obtain reproducible films. To remove the solvent vapor, due to the evaporating solvent of the spray, the chamber was continuously flushed with a flow of 10 L/min nitrogen gas. It was ensured that the flow of nitrogen did not disturb the cone-jet spray.

After preparation, films were imaged with JEOL SPM 4200. Imaging was done with tapping mode and low force on the cantilever (NSG10 cantilevers from NT-MDT, Russia). In all cases, images of 20×20 and $5 \times 5 \mu\text{m}$ were obtained. In some cases $1 \times 1 \mu\text{m}$ images were also taken. The $20 \times 20 \mu\text{m}$ images were used to determine the roughness average parameter as presented in Section 3.

Thickness profiles of the films were measured with the KLA Tencor P-15 Profiler. Infrared measurements on some films were performed with the JEOL JIR 7500 EM.

3. Results

The data for all samples of PVDF in DMF are presented in Table 1. The data concerning PVDF in acetone are shown in Table 2 and the data concerning VDF-oligomer sprayed in DMF are presented in Table 3. In all tables the sample number, concentration in weight percentage (wt%), conductivity ($\mu\text{S}/\text{cm}$), spray distance (cm), spray time (min), film thickness (nm), roughness average (nm), and density (g/cm^3) are given. All samples were sprayed at 20°C except two samples, 13 and 14, which were sprayed at 40°C . As far as it could be determined with infrared measurements, films prepared with acetone did

not contain any residual solvent. All films prepared with DMF contained DMF, although it was not possible to determine the exact amount. A number of films, especially samples 6, 31, 32, 33, and 37, were visibly wet and had clear impact of droplets. Roughness data of those samples and in some cases, thickness data could not be determined.

The amount of deposited material was calculated from the concentration, flow rate ($2 \mu\text{l}/\text{min}$ for DMF, $3 \mu\text{l}/\text{min}$ for acetone), and spray time. The film volume was calculated using thickness data and the diameter of the spherical deposit. From those two values the density follows. The error in the density is large, due to uncertainties in the amount of deposited material, radius, and, especially, film thickness. In certain cases, the films were extremely soft or not continuous on microscopic scale. If the density is placed between brackets, the error is expected to be $>50\%$. Density values are meant to give a general idea of how deposition conditions affect the film.

The sturdiest samples were made with high solvent conductivity and those samples demonstrate that the density of PVDF films is highest if sprayed with DMF. PVDF films sprayed with acetone seem to have a somewhat higher density than films made of VDF-oligomer. Determination of VDF-oligomer film thickness was hindered by the softness of most samples.

Table 1
Solutions of PVDF in DMF: sample number, concentration, and conductivity. Electrospray parameters: spray distance and time. Properties of the resulting films: thickness, roughness average, and density. The conductivity of the solutions was adjusted with ammonium nitrate

Sample	Concentration (wt%)	Conductivity ($\mu\text{S}/\text{cm}$)	Distance (cm)	Time (min)	Thickness (nm)	Roughness (nm)	Density (g/cm^3)
1	0.005	1.4	2	135	150	130	0.47
2	0.015	1.4	2	45	70	47	1.12
3	0.05	1.4	2	15	75	16	1.10
4	0.15	1.4	2	10	100	14	1.66
5	0.5	1.4	2	5	250	21	0.99
6 ^a	0.015	1.4	1.5	25	–	–	–
7	0.015	1.4	2.5	70	50	35	1.57
8	0.015	1.4	3	100	50	24	1.50
9	0.005	1.4	4	135	22	20	1.23
10	0.015	1.4	4	45	60	35	0.45
11	0.05	1.4	4	15	190	32	0.13
12	0.05	1.4	4	60	330	58	0.30
13 ^b	0.05	1.4	1.5	10	120	6.4	1.19
14 ^b	0.05	1.4	1	4.5	110	9.4	1.47
15	0.05	1.4	2	45	190	21	1.04
16	0.05	1.4	2	135	480	41	1.12
17	0.05	5.6	2	15	50	20	1.23
18	0.05	15	2	15	44	11	1.27
19	0.05	43	2	15	25	14	1.71

^a Film washed away from the substrate due to an excess of solvent.

^b Samples sprayed at 40°C instead of 20°C .

Table 2
Solutions of PVDF in acetone, electrospray parameters, and properties of the resulting films. The conductivity of the solutions was adjusted with ammonium nitrate

Sample	Concentration (wt%)	Conductivity ($\mu\text{S}/\text{cm}$)	Distance (cm)	Time (min)	Thickness (nm)	Roughness (nm)	Density (g/cm^3)
21	0.005	1.9	2	30	200	85	0.28
22	0.015	1.9	2	30	300	143	0.56
23	0.05	1.9	2	10	250	165	1.04
24	0.05	17	2	10	170	141	0.62
25	0.05	48	2	10	100	132	0.77

Table 3

Solutions of VDF-oligomer in DMF, electrospray parameters, and properties of the resulting films. The conductivity of the solutions was adjusted with ammonium nitrate

Sample	Concentration (wt%)	Conductivity ($\mu\text{S}/\text{cm}$)	Distance (cm)	Time (min)	Thickness (nm)	Roughness (nm)	Density (g/cm^3)
31 ^a	0.005	1.7	2	135	250	–	0.30
32 ^a	0.015	1.7	2	45	200	–	0.42
33 ^a	0.05	1.7	2	15	200	–	0.51
34	0.005	1.4	4	135	50	11	0.54
35	0.015	1.4	4	45	26	42	1.04
36	0.05	1.7	4	15	50	26	0.35
37 ^b	0.05	1.7	1	8	–	–	–
38	0.05	17	2	15	130	14	0.39
39	0.05	46	2	15	100	55	0.50

^a Film too rough to determine roughness average value.

^b Film washed away from the substrate due to an excess of solvent.

Thickness of the samples is not only a function of the amount of deposited material but also depending on spray conditions, such as conductivity, distance, and solvent. Different spray conditions give rise to a wider or narrower cone of droplets. The area covered by the spray can therefore differ extensively between experiments, which makes direct comparisons between film thicknesses difficult.

The roughness average (S_a) is the average height (z) difference, determined in the following way:

$$S_a = \frac{1}{MN} \sum_{k=0}^{M-1} \sum_{l=0}^{N-1} |z(x_k, y_l) - \mu| \quad (6)$$

and

$$\mu = \frac{1}{MN} \sum_{k=0}^{M-1} \sum_{l=0}^{N-1} z(x_k, y_l), \quad (7)$$

where M and N are the total number of pixels for the x and y axis, respectively. In all cases $20 \times 20 \mu\text{m}$ AFM images have been used to determine the roughness average.

To check the validity of Eqs. (1) and (3), they were plotted as function of the measured current. Both relationships fit the data fairly well; Eq. (3) gives the best fit, as can be seen in Fig. 2a. Given that the current scaling applies for all samples, it is safe to conclude that electrospray took place in the cone-jet mode and that Eqs. (2), (4), and (5) can be applied. With use of the measured current as input and the prefactors of Eq. (2), taking $f_b = 0.6$, the droplet size was calculated. The prefactors are not very important in this case, because the relative droplet size is enough to judge how change in droplet size affects the polymer film. There is a possibility, however, that Eq. (5) is valid. In that case Eqs. (2) and (4) will overestimate the size of the droplet.

The calculated droplet size can be found in Fig. 2b. The left scale is for the polymer particle size and the right scale is for the droplet size. The solid line is the whipping jet droplet size for DMF. For acetone this line lies slightly higher (dotted line). The filled circles are predictions of the droplet size as a function of the measured current. The crosses slightly displaced upward represent the droplet size for acetone. The displacement between DMF and acetone mainly reflects the difference in flow

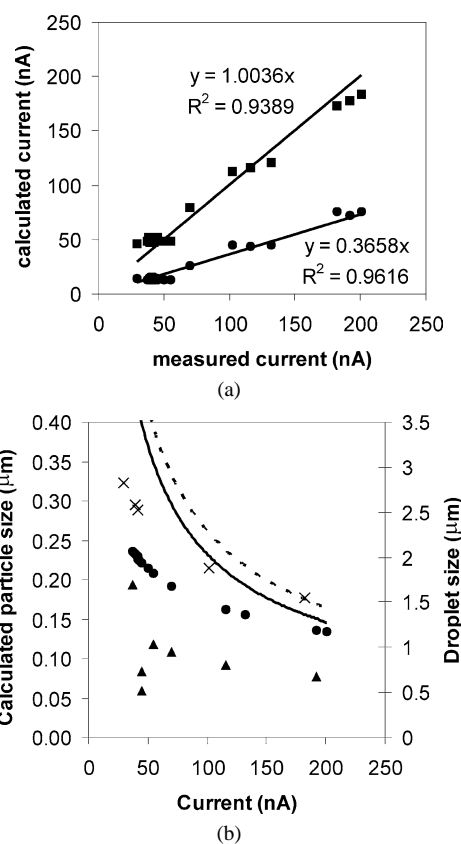


Fig. 2. (a) Validity check of the current scaling for Eq. (1) (filled squares) and Eq. (3) (filled circles). Both equations apply for the present data. Eq. (3) gives the best fit. (b) Droplet scaling with the current. The effect on the polymer particle size by increase of the current (or conductivity) and change of the concentration. Left scale: triangles: particle size of PVDF in DMF. The decrease of the particle size at 50 nA is due to a decrease in polymer concentration in the initial solution. Right scale: spheres: DMF droplet size; crosses: acetone droplet size; solid line: limit for varicose jet break-up for DMF (Eq. (5)); dotted line: limit for varicose jet break-up for acetone (Eq. (5)).

rate and is therefore a good illustration of its effect on droplet size. The triangles are an example of the expected polymer particle sizes in the case of PVDF in DMF. The triangles around a current of 50 nA illustrate the effect of the decrease in polymer concentration (0.15–0.005 wt%), whereas the decrease of the triangles with the current represent the effect of the increas-

ing conductivity (samples 3, 17–19). In all cases the varicose jet break-up applies, possibly except for the 1.5 μm acetone droplet at a current of about 200 nA (see Fig. 2b).

AFM images of various samples are presented along with the Discussion.

4. Discussion

4.1. Film morphology as a function of solvent: acetone and DMF

Solvent is an important parameter in electrospray. The stability of electrospray itself depends, to a large extent, on the properties of the solvent [10,36]. This means that in addition to polymer solubility, the solvent needs to have proper values for the relative permittivity, surface tension and in principle the density. Furthermore, the viscosity and conductivity of the solvent may need adjustment. Stable electrospray is a prerequisite to obtain well-defined polymer films.

If all requirements for a stable spray in combination with polymer solubility are met, the main effect of solvent on film morphology will be caused by the vapor pressure. This is illustrated with the effect of DMF (vapor pressure = 0.44 kPa) and acetone (vapor pressure = 30.8 kPa) on PVDF film morphology. Both samples, 3 (DMF) and 23 (acetone), are prepared under the same conditions and with the same amount of PVDF. The roughness average and the film thickness are much higher for the acetone sample than for the DMF sample (Tables 1 and 2). The surface of DMF sprayed film is much smoother than the acetone sprayed surface (Figs. 5c and 3a). Also the height

distribution of DMF sprayed film is much narrower (Figs. 4a and 6c).

In Table 4 the particle diameters are given, calculated with Eq. (4) for the acetone and DMF samples in Figs. 3 and 5. Although some of the DMF produced particles are smaller, DMF samples 4 and 5 produce larger polymer particles than any of the acetone samples. Nonetheless, almost all DMF samples result in a much smoother film, as follows from the comparison of Figs. 3 and 5 and of the roughness in Tables 1 and 3. The particle size alone can, therefore, not be the main cause of the much higher roughness for acetone spray. The smoothness must be due to an ability to flow, which translates into a difference in viscosity of the droplets at deposition for the DMF solution in comparison with the acetone solution.

No presence of acetone could be detected in the films sprayed with acetone. Certain films sprayed with DMF, however, were visibly wet (sample 6). Furthermore, VDF-oligomer, sprayed under the same conditions and with the same concentrations as PVDF, exhibited in a number of cases visibly wet film (compare VDF-oligomer samples 31, 32, and 33 with PVDF samples 1, 2, and 3). Because the interaction of DMF with VDF or with PVDF will be the same, the amount of DMF in the respective, depositing particles will be comparable. However, the much longer PVDF polymer molecules cause a much higher viscosity, which results in a moderate flow of the droplets and smooth film formation.

Comparing dry particles obtained with acetone and wet film obtained with DMF, the difference in vapor pressure is the cause behind the difference in observed morphology. Vapor pressure constitutes a window defining the range of control between a smooth, dense, and a rough, loose film. A low vapor pres-

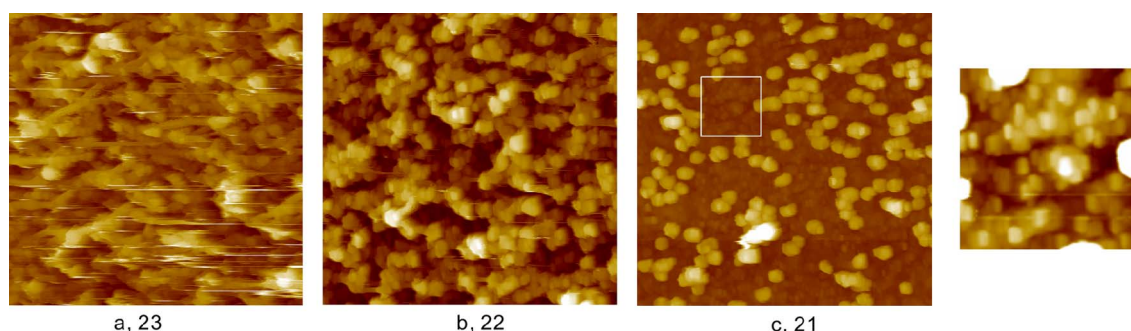


Fig. 3. Concentration dependence of PVDF sprayed in acetone (a) 0.05, (b) 0.015, and (c) 0.005 wt% with inset of zoomed area. The numbers refer to the sample number in sample description Table 2. All images are $5 \times 5 \mu\text{m}$, the inset is $1 \times 1 \mu\text{m}$.

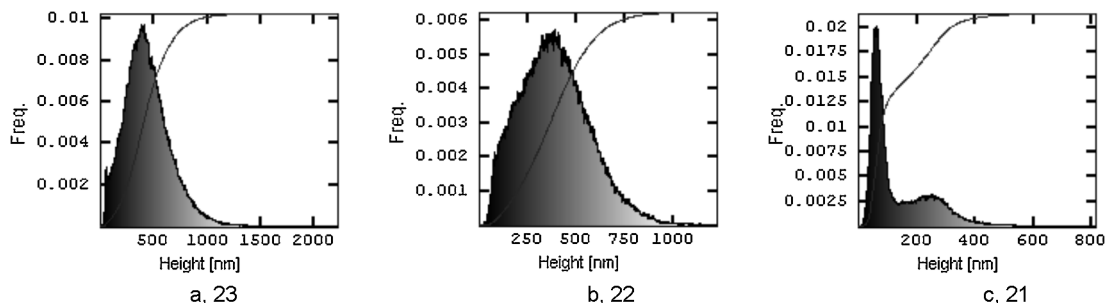


Fig. 4. Height distribution histograms for concentration dependence of PVDF sprayed in acetone (a) 0.05, (b) 0.015, and (c) 0.005 wt%. The numbers refer to the sample number in sample description Table 2.

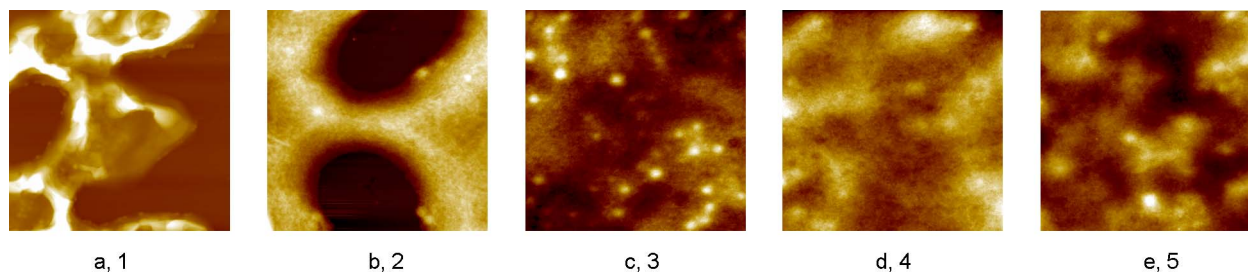


Fig. 5. Concentration dependence of PVDF sprayed in DMF (a) 0.005, (b) 0.015, (c) 0.05, (d) 0.15, and (e) 0.5 wt%. The numbers refer to the sample number in sample description Table 1. All images are $5 \times 5 \mu\text{m}$, except (a), which is $20 \times 20 \mu\text{m}$.

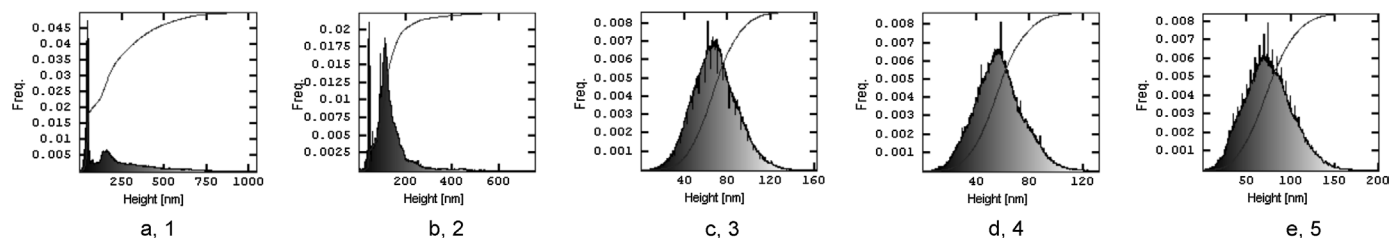


Fig. 6. Height distribution histograms for concentration dependence of PVDF sprayed in DMF (a) 0.005, (b) 0.015, (c) 0.05, (d) 0.15, and (e) 0.5 wt%. The numbers refer to the sample number in sample description Table 1.

Table 4

Calculated particle diameters (nm) of selected DMF (samples 1–5) and acetone (samples 21–23) samples sprayed under comparable conditions. The diameters have been calculated with Eq. (4) with use of the prefactor of Eq. (2) as described in the Introduction

Sample	Diameter DMF (nm)	Diameter acetone (nm)
1 and 21	61	73
2 and 22	84	103
3 and 23	118	172
4	194	–
5	250	–

sure solvent facilitates control; therefore DMF is a convenient solvent for electrospray. The amount of solvent present at deposition can be controlled, which will be shown in the following sections of this paper.

4.2. Changing the polymer/solvent ratio at deposition

The most straightforward way to control the polymer/solvent ratio of the droplet at deposition is with the initial concentration of the polymer. Various concentration ranges have been measured: PVDF in DMF, samples 1, 2, 3, 4, and 5; at 4 cm spray distance, samples 9, 10, 11, and 12; in acetone, samples 21, 22, and 23; for VDF, samples 31, 32, and 33, and for VDF at 4 cm, samples 34, 35, and 36. The AFM images of two concentration series are shown; PVDF in acetone, Fig. 3 presents the topographic images and Fig. 4 presents the height distribution histograms based on a $20 \times 20 \mu\text{m}$ area. PVDF in DMF is shown in Fig. 5 and the height distributions in Fig. 6.

The two series of AFM images (Figs. 3 and 5) show that the presence or absence of solvent in combination with changing concentration can have various effects. In the concentration series with acetone the solvent has evaporated before the droplet reaches the substrate. The result is a soft loosely packed film

consisting of only polymer particles and a clear effect of concentration is hardly noticeable. The only effect is an increase in the number of smaller particles with decreasing concentration (inset Fig. 3c). It is difficult to determine with these images if all particles become smaller as a function of decreasing concentration as expected from the calculations of the particle radius in Table 4, but such a decrease is confirmed in separate measurements in this laboratory (unpublished result) and found in Refs. [7,20]. The effect of the particle size on film roughness is illustrated in Fig. 7a. Only dry particles deposit on the substrate when sprayed with acetone and the roughness decreases with decreasing polymer particle size.

The concentration series of PVDF in DMF provides a completely different picture. There is a clear dependence of the surface morphology on the initial concentration. The low concentration solutions do not result in flat films, which can be seen in the height distributions of the respective surfaces. The sharp high peaks on the left in histogram Fig. 6a and 6b is silicon wafer substrate. The roughness average of the lowest concentration is high and its surface morphology (Fig. 5a) suggests that the impact of the solvent causes the roughness in this case. Apparently a lot of solvent is still present in the depositing droplets, washing away part of the deposit, exposing the substrate and roughening the polymer surface. In comparison, the equivalent sample of VDF-oligomer, sample 31, was too rough even to determine a roughness parameter with AFM due to the presence of DMF.

The film made with 0.015 wt% (Fig. 5b, sample 2) has regular oval areas of exposed substrate. It is unlikely that solvent impact causes such patterns. The effect is also found in sample 7 and under different conditions in sample 17 (Fig. 11). Probably the differences in surface energy of the PVDF–DMF mixtures with the silicon substrate in combination with the viscosity provide a situation where limited dewetting of the film is possible [40]. The idea is that dewetting is thermodynamically

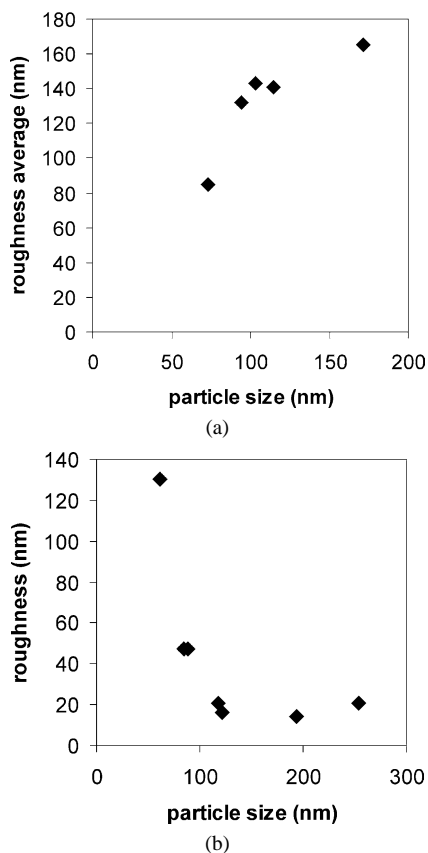


Fig. 7. (a) Film roughness as function of the particle size, sprayed with acetone. Only the particle size determines the roughness. (b) Film roughness as function of particle size resulting from the concentration; all droplet sizes are the same (samples 1–5, sprayed with DMF at 2 cm). The smallest particles show a much higher roughness due to a very low viscosity. The increase of the film roughness at the right side is due to an over-increase of viscosity.

favored for certain concentrations of PVDF in DMF on silicon wafer, possibly assisted by the charge on the droplets [41], but in most cases prevented by the viscosity and possibly also by the droplet impact.

The three higher concentrations (samples 3–5, Figs. 5c–5e) provide much smoother film, especially 0.15 wt% (Fig. 5d), which has the most narrow height distribution and the lowest roughness average. The density of the films as function of concentration is fairly constant around 1.10 g/cm^3 . The 0.15 wt% film density is even 1.66 g/cm^3 , which is close to the density of PVDF (1.74 g/cm^3) and is consistent with its smooth surface and narrow height distribution.

From Section 4.1 it is clear that DMF is present in the deposit and its amount decreases relative to the increasing initial concentration of PVDF. The effect of a relative decrease of DMF on the film roughness is presented in Fig. 7b. The film roughness is plotted as a function of the expected polymer particle size, which is entirely controlled by the initial polymer spray concentration. The droplet size of the spray is predicted to be the same for all concentrations, which means that for lower concentrations the polymer/solvent ratio at deposition will be lower and consequently the viscosity will also be lower. A low viscosity causes the film to be damaged, resulting in a high film roughness. With increasing concentration the viscosity in-

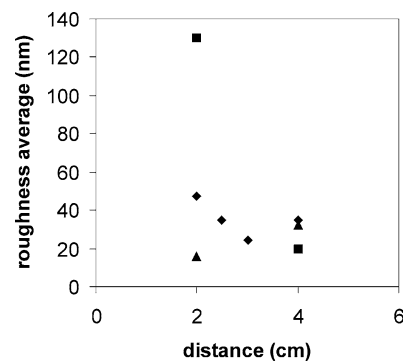


Fig. 8. Film roughness as function of the spray distance; PVDF in DMF, square: 0.005 wt%, diamond: 0.015 wt%, and triangle: 0.05 wt%. Increasing concentrations show a roughness average minimum at smaller distances. Since the distance only influences the evaporation of the solvent and therefore directly the viscosity, this graph shows how viscosity influences film roughness.

creases, decreasing the excessive flow and lowering the average roughness. The increase of the roughness on the right side of the graph is the result of an over-increase in viscosity, decreasing the flow even more and starting to reflect the increase of particle size like with acetone in Fig. 7a. Thus the difference in surface morphology in Fig. 7b is due to the change in viscosity, controlling the flow behavior of the PVDF–DMF mixture. The spread of the droplets on the substrate decreases with increasing initial PVDF concentration and the optimum concentration among the samples is 0.15 wt% PVDF in DMF.

The other concentration series mentioned at the beginning of this section show morphologies similar to those just described or show mixed behavior of partly dry particles smoothed more or less by the presence of solvent. An example of the latter is the concentration series of PVDF in DMF sprayed at 4 cm (samples 9, 10, 11, and 12) (not shown). The resulting films contain separate particles, however, the roughness average values are not as high as those of acetone. Samples 9, 10, 11, and 12, also serve as an example of an additional way to control the polymer/solvent ratio at deposition: changing the spray distance.

A good impression of how distance influences the surface morphology can be obtained with samples 2, 6, 7, 8, and 10 (no images shown), sprayed from 1.5 cm up to 4 cm distance with 0.015 wt% PVDF in DMF. They follow the same pattern as the concentration dependence in Fig. 5. At 1.5 cm, similar in appearance to sample 1, the amount of DMF in the deposit is too high for a smooth continuous film. The distances 2 cm (sample 2) and 2.5 cm show a regular hole-pattern in continuous film, as discussed before. At a distance of 3 cm, the roughness average is lowest and the film is similar to sample 3 (Fig. 5c). 4 cm spray distance results in a particle film although smoother than those sprayed with acetone.

The effect of spray distance on film roughness for these samples is shown in Fig. 8 in addition to two other concentrations. Although in this figure the exact location of the minima cannot be determined, it can be seen that the roughness minimum shifts to longer distance with lower concentration. Because for lower concentrations the amount of polymer in the droplet is smaller, more solvent needs to evaporate to obtain the optimum

ratio of polymer and solvent to form smooth film. In this case only the distance is directly responsible for the evaporation and if too much solvent evaporates the roughness increases again due to the fact that particles flow less, like in the extreme case of acetone.

Increasing the spray distance also increases the surface that will be covered by the spray. Therefore the combination of concentration and spray distance can be used to control the size of the covered area. The spraying time will increase with increasing distance, which may be a disadvantage.

Temperature can also be used to control the polymer/solvent ratio at deposition. A few films have been prepared at 40 °C with 0.05 wt%. Films made at 40 °C are smoother than films made at 20 °C (Fig. 9), which is likely due to the combination of the amount of residual DMF and a decrease in polymer viscosity induced by the higher temperature. The substrate was brought closer to the spray nozzle to obtain wet deposition conditions (at higher temperature the DMF evaporates faster, causing the films to be drier at 2 cm). As can be seen, 1.5 cm provides the most flat film with the most narrow height distribution. Roughness average indicates that sample 13, 0.05 wt%, 1.5 cm, and 40 °C, is the smoothest film in this study. The density of the films at 40 °C is similar to that of films prepared at 20 °C. Thus temperature, by influencing both vapor pressure and the viscosity directly, can be an important control parameter for desired film formation conditions.

By studying initial concentration, distance and temperature for any suitable solvent, optimal control over the polymer/solvent ratio at deposition can be obtained. The polymer/solvent ratio is an important tool to control the droplet viscosity within the window provided by the vapor pressure of the solvent.

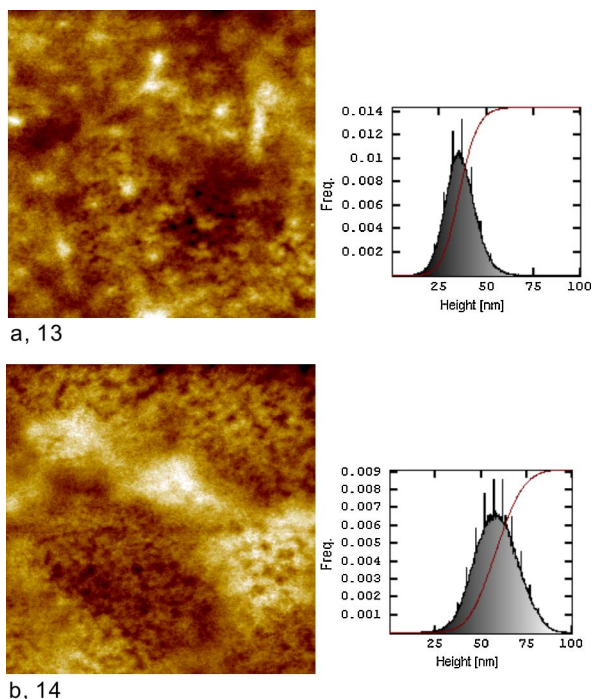


Fig. 9. PVDF sprayed in DMF at 40 °C (a) 1.5 and (b) 1 cm. The numbers refer to the sample number in sample description Table 1. Both images are 5 × 5 μm.

4.3. Other factors influencing film quality

An additional concentration effect that can be found for acetone (Fig. 3) and also for DMF at 4 cm spray distance is a shifting particle size distribution. The ratio of smaller particles over larger particles is increasing, whereas the decrease of particle size is much less apparent, with decreasing concentration. A bimodal size distribution is expected from the cone-jet break-up [15]. In addition, the size distribution will broaden due to charge and liquid release of droplets reaching the Rayleigh limit [42]. The Rayleigh limit will not depend on polymer concentration, but only on droplet size and charge. Droplets of concentrated solutions might reduce the Rayleigh limit induced stress by expelling only charged solvent, increasing the entanglement of the polymers in the droplet. One should keep in mind that concentrations in the droplet are higher than in the initial solution due to the continuous evaporation of liquid from the droplet. Polymers in the initial solution will be in a dilute solution regime, and barely interact with each other. Concentrations within a droplet might be close to or in the concentrated solution regime, where polymers form a network. If the initial concentration is decreased, the concentration in the droplet decreases too. The chance for a single polymer molecule to get entangled with other polymers will decrease. Thus it will be more likely that the Rayleigh limit will cause polymers to be expelled from the droplet together with the small solvent droplets. This will result in a larger quantity of small polymer particles.

The same effect as observed for the acetone samples is expected to occur with the DMF samples. However, due to the smooth films, it is impossible to determine to what extent small particles are formed. In any case, the presence of very small polymer particles will improve the smoothness of the film, as long as the viscosity at deposition is controlled.

The amount of polymer in a sprayed film is a function of the spraying time. Samples 3, 15, and 16 are sprayed under the same conditions, only the spraying time differs. The density is not affected. The absolute roughness average increases, but the ratio of the roughness average with the film thickness decreases with spraying time (or with film thickness). Although spraying time appears to improve the relative smoothness, the result also shows that one should be careful when comparing the absolute roughness average of samples of different film thickness.

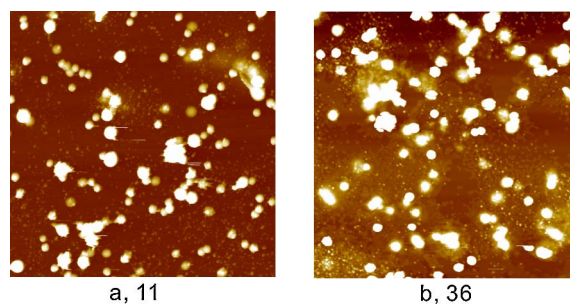


Fig. 10. (a) 0.05 wt% PVDF in DMF sprayed at 4 cm and (b) 0.05 wt% VDF-oligomer in DMF sprayed at 4 cm. The numbers refer to the sample description Tables 1 and 3, respectively. Both images are 5 × 5 μm.

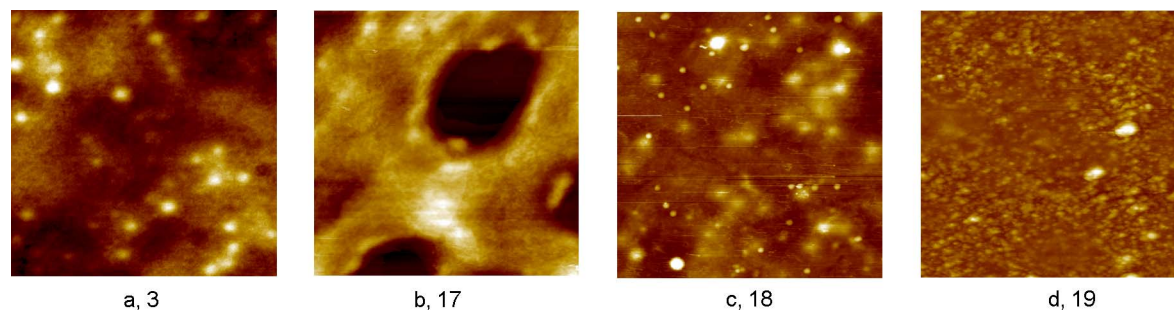


Fig. 11. Conductivity dependence of PVDF (0.05 wt%) sprayed in DMF (a) 1.4, (b) 5.6, (c) 15, and (d) 43 $\mu\text{S}/\text{cm}$. The numbers refer to the sample number in sample description Table 1. All images are $5 \times 5 \mu\text{m}$.

4.4. Molecular size and film morphology

At 2 cm spray distance the VDF-oligomer deposition is too wet to form continuous films. Even though the concentration in sample 3, PVDF, and sample 33, VDF-oligomer, is the same, the VDF-oligomer droplets have a lower viscosity and are washed off from the substrate. At 4 cm spray distance, 0.05 wt% VDF-oligomer is strikingly similar to 0.05 wt% PVDF in DMF in appearance and height distribution (samples 36 and 11, see Fig. 10) and also the roughness average is of the same order (samples 26 and 32, respectively). The compound/solvent ratio at deposition should be comparable, but the VDF-oligomer droplets are expected to spread more easily than the PVDF-polymer droplets.

It is known that viscosity depends on polymer chain length. Since viscosity is also concentration dependent, much higher concentrations have to be used for the short VDF-oligomer to obtain viscosity values similar to those of PVDF-samples. These concentrations might be reached by adjusting the initial concentration or also by adjusting temperature or spray distance. The latter is illustrated with the spray result of VDF-oligomer at a spray distance of 4 cm in comparison to 2 cm. However, in the case of the VDF-oligomer, the chain length is so short that it is not expected to form an interconnected network under any circumstance. Therefore, a concentrated regime in the sense of polymer solution theory does not exist anymore for a molecule the size of a VDF-oligomer. Therefore the viscosity behavior and the resulting spreading behavior on the substrate might not be sufficient for the VDF-oligomer to form smooth films, despite adjustments in concentration, distance, or temperature. The latter will certainly be the case for even smaller molecules. Thus the manipulation of film smoothness by means of the viscosity is only applicable for polymers, which are of sufficient length.

4.5. Conductivity and film morphology

Conductivity and also flow rate have a significant effect on the droplet size according to the scaling relationships mentioned in the Introduction. Since in this study flow rate is used for spray stability control, it is not separately studied for the control of droplet size. It is known from literature that a decrease of nozzle diameter increases the flow-rate range for a stable cone-jet spray [2,14]. This facilitates the use of flow rate

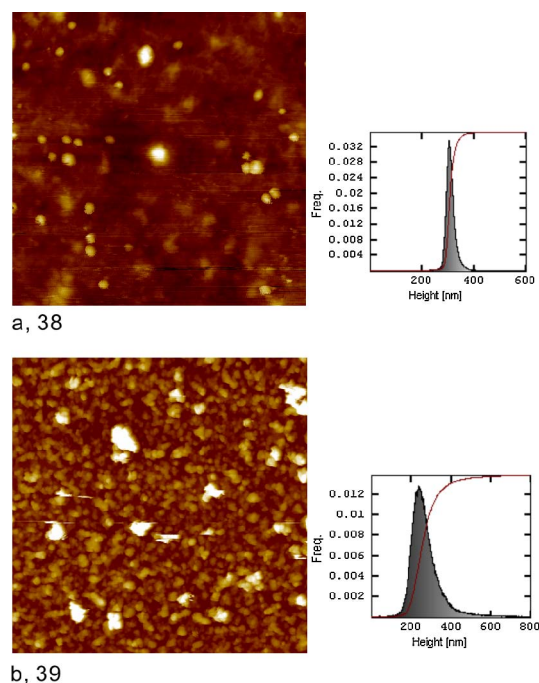


Fig. 12. Conductivity dependence of VDF-oligomer (0.05 wt%) sprayed in DMF (a) 17 and (b) 46 $\mu\text{S}/\text{cm}$. The numbers refer to the sample number in sample description Table 3. All images are $5 \times 5 \mu\text{m}$. The height distribution histograms are of the respective $20 \times 20 \mu\text{m}$ images.

instead of conductivity as a control parameter if desirable, since their effect on the droplet size follows in both cases from the scaling laws. The dependence of droplet size on the conductivity is described in the Introduction by Eqs. (2) and (4) [9,10,15] and an example of decreasing particle size as a function of increasing conductivity is shown in Fig. 2.

The resulting film morphology due to increased conductivity can be seen for samples 18 and 19 with a conductivity of 15 and 43 $\mu\text{S}/\text{cm}$, respectively (Fig. 11). The increase of conductivity increases the smoothness (and possibly the density) of all films, also for acetone and for VDF-oligomer. For example, VDF-oligomer with a conductivity of 17 $\mu\text{S}/\text{cm}$ (Fig. 12) produces one of the smoother films, in particular in comparison with the low-conductivity samples of VDF-oligomer (Table 3). Furthermore, it can be observed that increased conductivity decreases the particle size, as expected (compare Fig. 11d and Fig. 3 with Fig. 2b). If droplets become even smaller evaporation increases and almost dry particles are obtained. The latter can be seen

for both PVDF and VDF-oligomer in DMF for $\sim 45 \mu\text{S}/\text{cm}$ (Figs. 11 and 12).

The observations in the foregoing paragraph illustrate the effects of an increase in the conductivity on film morphology. In Fig. 2b it can be seen how the conductivity decreases the droplet size of the spray. The direct result of a droplet decrease is a decrease of the polymer particle size (Fig. 2b) and this results in a reduction of film roughness. In addition, smaller droplets will evaporate faster and increase the polymer/solvent ratio in the droplet; therefore, the viscosity increases with an increase of the conductivity.

In Fig. 13 both the decrease of particle size (squares) and the change of the roughness parameter (triangles) as function of the conductivity are presented for PVDF in DMF. The increase of the roughness parameter for $5 \mu\text{S}/\text{cm}$ in comparison with $1.4 \mu\text{S}/\text{cm}$, is due to the appearance of empty circular areas in the former film (see Fig. 11b), caused by dewetting as discussed previously. The lowest roughness value can be found for $15 \mu\text{S}/\text{cm}$ in Fig. 13, reflecting the optimum combination of particle size and droplet viscosity in the dataset. For $43 \mu\text{S}/\text{cm}$ the particle size is again smaller, but the viscosity has become too high, preventing a decrease in roughness; the same occurred as function of the concentration (see Fig. 7b). On the other hand, the film roughness with acetone, entirely depending on the particle size, still continues to decrease at $48 \mu\text{S}/\text{cm}$ (Table 2); a film roughness which is still high in comparison to DMF due to the total absence of solvent in the particles. Thus

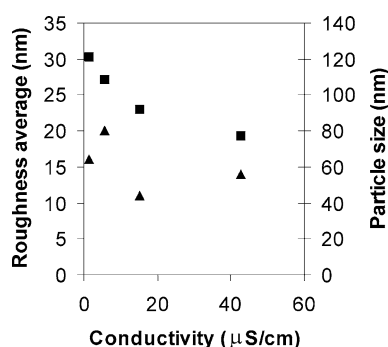


Fig. 13. Film roughness as function of the conductivity (or current), samples 0.05 wt% PVDF in DMF; triangle: roughness average (left axis); square: particle size (right axis). Increase of conductivity causes an increase of viscosity first decreasing the film roughness, until viscosity slowly becomes too high causing the roughness to increase again. The roughness at $5 \mu\text{S}/\text{cm}$ is higher due to a dewetting effect as discussed in the text in Section 4.2.

conductivity controls the droplet size, which in the case of DMF controls both the particle size and the polymer/solvent ratio. The optimum combination of both provides the smoothest film.

In the case of acetone, the deposit is already dry and only the particle size determines the smoothness of the film. Interestingly a bimodal distribution can be found in the height distribution profiles of increasing conductivity for the acetone solutions (see Fig. 14). Instead of the main distribution slowly changing to lower size differences, reflecting the decrease of particle size, the distribution peak of larger size differences is slowly replaced by a distribution of smaller size differences. This is an effect very similar to the increase of small particles as a function of the concentration, but in this case it is driven by an increase in charge on the droplet. Since acetone evaporates quickly, an increase in conductivity causes a droplet to reach the Rayleigh limit more often. More polymers are likely to be ejected in small droplets from the main droplet, when discharge takes place. The particle representing the main droplet will also deposit and it will reduce in size as a function of the conductivity. This is in accordance with the behavior of the height distributions in Fig. 14.

In applications, wet deposition as with DMF may be undesirable, for example because of solvent sensitive substrates. The preparation of dry film by means of increased conductivity in DMF may be an option in such cases. Increased conductivity tends to give sturdier films than fast evaporating solvents such as acetone. On the other hand, those films will contain a salt or other agent to increase conductivity. If that is undesirable, decreasing flow rate can also be used to decrease particle size in the film, which can be adjusted within a set range of spray stability just like the conductivity. However, use of conductivity will allow a higher film production rate.

The use of conductivity to control the droplet size completes the picture of control over the surface morphology of polymer thin films. Even though other solvent properties can be used to change droplet size, in general they cannot be changed without also changing additional solvent properties. Changing the solvent is often not desirable due to its key role in electro-spray stability and polymer solubility. Even the surface tension is mainly dependent on the solvent. A large difference in time scale exists between the fast cone-jet process and the much slower static equilibrium surface tension caused by surfactants. Therefore the addition of surfactants to the sprayed solution does not allow for straightforward manipulation of the short-timescale cone-jet

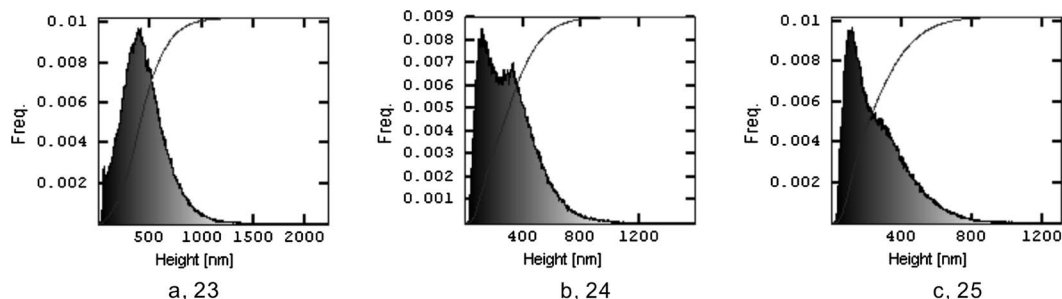


Fig. 14. Height distribution histograms for conductivity dependence of PVDF sprayed in acetone (a) 1.9, (b) 17, and (c) $48 \mu\text{S}/\text{cm}$. The numbers refer to the sample number in sample description Table 2.

process. A good example of the ineffectiveness of surfactants can be found in Ref. [33]. The viscosity of the spray solution can most likely range up to 10 mPa s without any significant effect on the conclusions of this paper and possibly even to 20 mPa s, as discussed in the Introduction. Of course, modifying the spray viscosity does affect the viscosity at deposition, and this might have to be taken into account when tuning the polymer/solvent ratio at deposition. Nevertheless, because of the use of dilute solutions, the direct increase of viscosity will be a relatively small effect in comparison with the viscosity increase due to the evaporation of the solvent. Very high values of viscosity will favor electrospinning, which produces a different morphology altogether.

5. Conclusions

Solvent is the key parameter for the production of polymer thin films with electrospray. The solvent defines the framework of electrospray parameters for a stable cone-jet. It also has to be a good solvent for the polymer. In addition the solvent has a strong influence on polymer film morphology. Choosing a solvent with a low vapor pressure allows easy control over deposition conditions and the resulting film. It provides a relatively large window to adjust parameters which control the viscosity of the deposit to find the desired combination of conditions for optimal, smooth film production.

The polymer/solvent ratio at deposition is directly linked with the viscosity. It can be controlled with the initial spray concentration and the amount of solvent evaporating in flight. The evaporation is controlled with the vapor pressure, droplet size, spray distance, and temperature. Temperature also directly affects polymer viscosity.

Polymer size determines the viscosity of the deposit. Short polymers will need high concentrations to obtain levels of viscosity similar to longer polymers. If molecules become too small, the solution property of adjustable viscosity will be lost. Tuning film morphology with the adjustment of the viscosity is therefore limited to polymer solutions.

Two convenient parameters for control of the droplet size have been obtained with theoretical cone jet models; the flow rate and the conductivity. The change of the droplet size, controlled by the conductivity, gives rise to various polymer film morphologies. Droplet size is directly linked to the size of the depositing particle. Smaller particles will result in a smoother film. In addition the droplet size affects the rate of evaporation of the solvent, therefore also affecting the polymer/solvent ratio. With the use of conductivity smooth polymer films were made as thin as 25 nm. The combination of conductivity and temperature adjustment may be promising for even thinner films.

Optimization of polymer film with the foregoing approach is straightforward, although it can be time consuming, due to the large number of interdependent parameters. It can be further complicated due to the fact that cone-jet stability also depends on several of the same parameters.

In electrospray, the combination of control over the droplet size and droplet viscosity with conductivity, flow rate, polymer

concentration, polymer size, temperature, and spray distance, provides a versatile and comprehensive means of control over polymer film morphology.

Acknowledgment

This work was supported by the Integrated Industry Academia Partnership (IIAP), Kyoto University International Innovation Center.

References

- [1] G. Taylor, Proc. Roy. Soc. London A 280 (1964) 383.
- [2] M. Cloupeau, B. Prunet-Foch, J. Electrostat. 22 (1989) 135.
- [3] M. Cloupeau, B. Prunet-Foch, J. Electrostat. 25 (1990) 165.
- [4] M. Cloupeau, B. Prunet-Foch, J. Aerosol Sci. 25 (1994) 1021.
- [5] C.M. Whitehouse, R.N. Dreyer, M. Yamashita, J.B. Fenn, Anal. Chem. 57 (1985) 675.
- [6] J.M. Grace, J.C.M. Marijnissen, J. Aerosol Sci. 25 (1994) 1005.
- [7] D.-R. Chen, D.Y.H. Pui, S.L. Kaufman, J. Aerosol Sci. 26 (1995) 963.
- [8] A.M. Ganan-Calvo, J. Fluid Mech. 335 (1997) 165.
- [9] A.M. Ganan-Calvo, Phys. Rev. Lett. 79 (1997) 217.
- [10] A.M. Ganan-Calvo, J. Davila, A. Barrero, J. Aerosol Sci. 28 (1997) 249.
- [11] A. Barrero, A.M. Ganan-Calvo, J. Davila, A. Palacio, E. Gomez-Gonzalez, Phys. Rev. E 58 (1998) 7309.
- [12] A. Barrero, A.M. Ganan-Calvo, J. Davila, A. Palacio, E. Gomez-Gonzalez, J. Electrostat. 47 (1999) 13.
- [13] K. Tang, A. Gomez, Phys. Fluids 6 (1994) 2317.
- [14] K. Tang, A. Gomez, J. Colloid Interface Sci. 184 (1996) 500.
- [15] R.P.A. Hartman, D.J. Brunner, D.M.A. Camelot, J.C.M. Marijnissen, B. Scarlett, J. Aerosol Sci. 31 (2000) 65.
- [16] A.A. van Zomeren, E.M. Kelder, J.C.M. Marijnissen, J. Schoonman, J. Aerosol Sci. 25 (1994) 1229.
- [17] C.H. Chen, M.H.J. Emond, E.M. Kelder, B. Meester, J. Schoonman, J. Aerosol Sci. 30 (1999) 959.
- [18] C.H. Chen, E.M. Kelder, J. Schoonman, J. Eur. Ceram. Soc. 18 (1998) 1439.
- [19] V.N. Morozov, T.Y. Morozova, N.R. Kallenbach, Int. J. Mass. Spectrom. 178 (1998) 143.
- [20] R. Festag, S.D. Alexandratos, K.D. Cook, D.C. Joy, B. Annis, B. Wunderlich, Macromolecules 30 (1997) 6238.
- [21] J. Sakata, M. Mochizuki, Thin Solid Films 195 (1991) 175.
- [22] N. Fujitsuka, J. Sakata, Y. Miyachi, K. Mizuno, K. Ohtsuka, Y. Taga, O. Tabata, Sens. Actuators A 66 (1998) 237.
- [23] B. Hoyer, G. Sorensen, N. Jensen, D.B. Nielsen, B. Larsen, Anal. Chem. 68 (1996) 3840.
- [24] E.H. Sanders, K.A. McGrady, G.E. Wnek, C.A. Edmondson, J.M. Mueller, J.J. Fontanella, S. Suarez, S.G. Greenbaum, J. Power Sources 129 (2004) 55.
- [25] N. Dam, M.M. Beerbom, J.C. Braunagel, R. Schlaf, J. Appl. Phys. 97 (2005) 0249091.
- [26] H. Fong, I. Chun, D.H. Reneker, Polymer 40 (1999) 4585.
- [27] R. Jaeger, H. Schoenherr, G.J. Vancso, Macromolecules 29 (1996) 7634.
- [28] C.J. Buchko, L.C. Chen, Y. Shen, D.C. Martin, Polymer 40 (1999) 7397.
- [29] R.G. Kepler, in: H.S. Nalwa (Ed.), Ferroelectric Polymers, Dekker, New York, 1995, p. 183.
- [30] K.L. Choy, W. Bai, Thin Solid Films 372 (2000) 6.
- [31] C. Berkland, D.W. Pack, K. Kim, Biomaterials 25 (2004) 5649.
- [32] I. Uematsu, H. Matsumoto, K. Morota, M. Minagawa, A. Tanioka, Y. Yamagata, K. Inoue, J. Colloid Interface Sci. 269 (2004) 336.
- [33] K. Morota, H. Matsumoto, T. Mizukoshi, Y. Konosu, M. Minagawa, A. Tanioka, Y. Yamagata, K. Inoue, J. Colloid Interface Sci. 279 (2004) 484.
- [34] R. Saf, M. Goriup, T. Steindl, T.E. Hamedinger, D. Sandholzer, G. Hayn, Nat. Mater. 3 (2004) 323.
- [35] M. Cloupeau, J. Aerosol Sci. 25 (1994) 1143.
- [36] R.P.A. Hartman, D.J. Brunner, D.M.A. Camelot, J.C.M. Marijnissen, B. Scarlett, J. Aerosol Sci. 30 (1999) 823.

[37] F. Ravera, L. Liggieri, R. Miller, *Colloids Surf. A* 175 (2000) 51.

[38] M.J. Schick, *Nonionic Surfactants*, Dekker, New York, 1967.

[39] J.M. Lopez-Herrera, A.M. Ganan-Calvo, M. Perez-Saborid, *J. Aerosol Sci.* 30 (1999) 895.

[40] R. Khanna, A. Sharma, G. Reiter, *EPJdirect* 2, 2000, E2.

[41] L.-T. Lee, M.D.C.V. Da Silva, F. Galembeck, *Langmuir* 19 (2003) 6717.

[42] P. Kebarle, Y. Ho, in: R.B. Cole (Ed.), *Electrospray Ionization Mass Spectrometry*, Wiley, New York, 1997, p. 3.